British Journal of Pharmacology (1996) 117, 639-646

Differences in the operational characteristics of the human recombinant somatostatin receptor types, sst_1 and sst_2, in mouse fibroblast (Ltk^-) cells

Sandra W. Castro, *Gary Buell, [1]Wasyl Feniuk & Patrick P.A. Humphrey

Glaxo Institute of Applied Pharmacology, University of Cambridge, Department of Pharmacology, Tennis Court Road, Cambridge, CB2 1QJ and *Glaxo Institute for Molecular Biology SA, 14 chemin des Aulx-Case Postale 674, 1228 Plan-les-Ouates, Geneva, Switzerland

1 The human recombinant somatostatin (SRIF) receptors, sst_1 and sst_2, have been stably expressed in mouse fibroblast (Ltk^-) cells. Two stable clones, LSSR1/20 and LSSR11/13, expressing sst_1 and sst_2 receptors, respectively, have been used to characterize these receptor types using radioligand binding assays as well as measurements of changes in extracellular acidification rates using microphysiometry.

2 [^{125}I]-[Tyr^{11}]-SRIF bound to sst_1 and sst_2 receptors expressed in Ltk^- cells with high affinity, K_d values being 1.52 nM and 0.23 nM, respectively.

3 In Ltk^- cells expressing sst_1 receptors, SRIF, SRIF-28, [D-Trp^8]-SRIF and CGP 23996 all displaced [^{125}I]-[Tyr^{11}]-SRIF binding with high potency (IC_{50} values of 0.43-1.27 nM) whilst seglitide, BIM-23027, BIM-23056 and L-362855 were either weak inhibitors of binding or were ineffective.

4 In contrast MK-678 (seglitide) and BIM-23027 were the most potent inhibitors of [^{125}I]-[Tyr^{11}]-SRIF binding in Ltk^- cells expressing sst_2 receptors with IC_{50} values of 0.014 and 0.035 nM, respectively.

5 SRIF and a number of SRIF agonists, including seglitide and BIM-23027, caused concentration-dependent increases in extracellular acidification rates in Ltk^- cells expressing sst_2 receptors but not in Ltk^- cells expressing sst_1 receptors. The maximum increase in acidification rate produced by SRIF was $11.3 \pm 0.7\%$ above baseline (0.1-0.28 pH unit min^{-1}). The relative potencies of the SRIF agonists examined in causing increases in extracellular acidification rates in Ltk^- cells expressing sst_2 receptors correlated well with their relative potencies in inhibiting [^{125}I]-[Tyr^{11}]-SRIF binding ($r = 0.94$).

6 The increase in extracellular acidification produced by SRIF was markedly inhibited by pretreatment of cells with pertussis toxin (100 ng ml^{-1}) indicating the involvement of pertussis toxin-sensitive G proteins.

7 SRIF (1 μM) had no effect on basal cyclic AMP levels in Ltk^- cells expressing sst_1 or sst_2 receptors nor did it inhibit forskolin stimulated increases in cyclic AMP levels in either cell type.

8 The results from the present study describe the operational characteristics of human sst_2 receptors expressed in Ltk^- cells where receptor activation causes increases in extracellular acidification rates. This receptor is coupled to a pertussis toxin-sensitive G protein. In contrast, activation of sst_1 receptors, at a similar transfection density, did not cause increases in extracellular acidification rates.

Keywords: Somatostatin receptors; microphysiometry; extracellular acidification; SRIF analogues

Introduction

Somatostatin (SRIF; somatotropin release inhibitory factor) is a neuropeptide which acts as a hormone and neurotransmitter in the peripheral and central nervous systems (Reichlin, 1983). The diverse effects of SRIF include the inhibition of the release of other hormones, such as insulin and growth hormone, the inhibition of motility in the gut, antisecretory actions as well as reductions in cardiac contractility (Reichlin, 1983; McKeen *et al.*, 1994; Feniuk *et al.*, 1995). In the central nervous system, however, SRIF has been found to stimulate the release of a number of other neurotransmitters, including 5-hydroxytryptamine (5-HT), dopamine and acetylcholine (Epelbaum, 1986).

Prior to the advent of receptor gene cloning, a number of studies suggested the existence of two somatostatin receptor types, $SRIF_1$ and $SRIF_2$ (Reubi, 1984; Raynor & Reisine, 1989; Raynor *et al.*, 1991). This classification was based on the difference in affinities of the cyclohexapeptides, MK-678 (seglitide) or SMS-201995 (octreotide), for two SRIF binding sites, with $SRIF_1$ sites having a much higher affinity for seglitide and octreotide than $SRIF_2$ sites. In functional studies, SRIF receptors have been found to be coupled to a variety of different transduction systems, including the inhibition of adenylyl cyclase (Jakobs *et al.*, 1983), voltage-dependent Ca^{2+} channels (Lewis *et al.*, 1986) and the mobilization of intracellular Ca^{2+} (Koch *et al.*, 1985). SRIF receptors have also been shown to be coupled to the stimulation of voltage-dependent K^+ channels (Yamashita *et al.*, 1987) and protein phosphatases (Liebow *et al.*, 1989). Many of these effects involve pertussis toxin-sensitive G proteins. In addition, SRIF has been shown to inhibit proliferation of AR4-2J pancreatic cells (Viguerier *et al.*, 1989) and to inhibit the Na^+/H^+ exchanger in enteric endocrine cells via a pertussis toxin-insensitive pathway (Barber *et al.*, 1989).

Genes for five distinct somatostatin receptor types, sst_1-sst_5, have now been cloned (for review, see Hoyer *et al.*, 1995). On the basis of sequence similarity and radiolabelled ligand binding studies, the protein products of the sst_2, sst_3 and sst_5 genes appear to belong to the $SRIF_1$ class having high affinity for MK-678, whilst the protein products of the sst_1 and sst_4 genes have little or no affinity for MK-678, placing them in the $SRIF_2$ class (Hoyer *et al.*, 1995). Each of these recombinant receptor types have been expressed in a number of different cell

[1] Author for correspondence.

lines, and all have been found to couple negatively to adenylyl cyclase and, to varying degrees, positively to phospholipase C, leading to Ca^{2+} mobilization (Kaupmann *et al.*, 1993; Akbar *et al.*, 1994; Patel *et al.*, 1994). However, it is not known how important these pathways are for transducing the effects of SRIF receptor activation in whole tissues.

A number of putatively selective compounds have been identified; BIM-23027 is reportedly selective for the sst_2 receptor, BIM-23056 for the sst_3 receptor and L-362,855 for the sst_5 receptor (Raynor *et al.*, 1993a,b). These peptides have been used in radioligand binding assays, but have yet to be reported as having functional activity at their respective recombinant receptors. To date, there are no selective peptides reported for sst_1 and sst_4 receptors. In the present study, we have expressed the human recombinant sst_1 and sst_2 receptors in mouse fibroblast (Ltk^-) cells. We have used these putatively selective compounds and a number of other SRIF analogues to assess their binding characteristics as well as their functional activities at these two SRIF receptor types, using microphysiometry to measure extracellular acidification rates. The effect of SRIF on basal as well as forskolin-stimulated adenylyl cyclase activity is also described. Preliminary accounts of some of these findings have been presented to the British Pharmacological Society (Castro *et al.*, 1994; 1995).

Methods

Cloning of the human sst_1 and sst_2 receptor genes

Human cDNAs for the respective sst_1 and sst_2 receptors were cloned by hybridization and PCR. The sst_1 receptor cDNA was isolated from a lambda library of human foetal brain cDNAs (Strategene, λ ZAP II). Hybridization probes were generated from the previously published sequence (Yamada *et al.*, 1992). The 3500 bp cDNA insert for the sst_1 receptor was transfected into plasmid pBSK (Strategene) by *in vivo* excision and sequenced by exonuclease deletion (Henikoff, 1984). A 1400 bp PstI–NarI fragment, containing the entire region for expression of the sst_1 receptor, was subcloned into pBKS (Strategene) for all further manipulations.

The cDNA for the sst_2 receptor was isolated by PCR directly from human genomic DNA. Oligonucleotide primers, based on the published sequence (Yamada *et al.*, 1992), were used to amplify a 1230 base pair fragment containing the translated portion of the gene. This fragment was blunt ligated into the EcoRV site of pBSK and sequenced by dye terminator chemistry with specific oligonucleotides. Expression plasmids for the two receptor types were generated by blunt ligation of fragments from the pBluescript intermediates into EcoRV-linearized pBGDRdhfrNeo3 (Buell *et al.*, 1992).

Cell culture

Mouse fibroblast Ltk^- cells (ECACC, Porton Down, U.K.) were grown in Dulbecco's Modified Eagles Medium (DMEM) supplemented with 10% foetal calf serum. Transfected cells were selected in media containing 600 $\mu g\ ml^{-1}$ G418 and clonal cell lines were maintained in media containing 500 $\mu g\ ml^{-1}$ G418.

Expression of human sst_1 and sst_2 receptors

The expression vector, pBGDRdhfrNeo3, containing the cDNA for either the human sst_1 or sst_2 receptor, was stably transfected into mouse fibroblast (Ltk^-) cells by the calcium phosphate precipitation method (Page, 1988). Clonal cell lines were isolated by dilution cloning and were screened for expression of either sst_1 or sst_2 receptors using [^{125}I]-[Tyr^{11}]-SRIF. Two cell lines, LSSRI/20 and LSSRII/13, expressing the human sst_1 and sst_2 receptors, respectively, were chosen for further analysis.

Cell membrane preparation

Cells were homogenized in assay buffer (50 mM Tris-HCl (pH 7.4), 5 mM $MgCl_2$, 10 $\mu g\ ml^{-1}$ leupeptin, 1 $\mu g\ ml^{-1}$ soyabean trypsin inhibitor, 0.2 $mg\ ml^{-1}$ bacitracin and 0.5 $\mu g\ ml^{-1}$ aprotinin) in a Dounce glass: glass homogenizer (50 strokes, 4°C). The homogenate was centrifuged at 500 *g* for 10 min at 4°C and the supernatant spun at 20,000 *g* for 30 min at 4°C. The resultant pellet was resuspended in cold assay buffer and stored in 1 ml aliquots at −70°C.

Radiolabelled ligand binding assays

Cell membranes (20–30 μg protein) were incubated with 0.03 nM [^{125}I]-[Tyr^{11}]-SRIF and increasing concentrations of SRIF or a SRIF analogue for 90 min at room temperature. Non-specific binding was defined with 1 μM SRIF. The assay was terminated by rapid filtration through Whatman GF/C glass fibre filters soaked in 0.5% polyethylenimine (PEI), followed by 3 × 3 ml washes of 50 mM Tris-HCl pH 7.4 containing 5 $mg\ ml^{-1}$ bovine serum albumin (BSA). Radioactivity in the filters was determined using a Canberra Packard Cobra II Auto-γ counter. Data were analysed by non-linear regression using the curve-fitting programmes EBDA and LIGAND (Munson & Rodbard, 1980; McPherson, 1985).

Cyclic AMP assays

Cells were plated out in 24-well cell culture plates at about 2.5×10^5 cells per well, 48 h prior to the experiment. After washing twice with serum-free medium, cells were pre-incubated with medium containing 0.5 mM isobutylmethylxanthine (IBMX) for 30 min, followed by a 1 min incubation with medium containing 10 mM forskolin in the presence or absence of 1 μM SRIF. The assay was terminated by the addition of 300 μl 0.5 M trichloroacetic acid which was subsequently removed by washing with 3 × 2 ml water-saturated diethyl ether. A 200 μl aliquot of the washed sample was neutralised with 50 μl 60 mM $NaHCO_3$ and the amount of adenosine 3′:5′-cyclic monophosphate (cyclic AMP) present was analysed using [^{125}I]-cyclic AMP radioimmunoassay kit (RPA 509; Amersham International, U.K.).

Protein assay

Protein from cell membrane preparations and cyclic AMP assay samples was determined with a bicinchoninic acid (BCA) Protein Assay kit.

Measurement of cell extracellular acidification rates

Cells were seeded into Cytosensor microphysiometer cups (Molecular Devices, Menlow Park, California, U.S.A.) at a density of 7.5×10^5 cells per cup, 18–24 h prior to the experiment. Bicarbonate-free DMEM (pH 7.4) containing 0.2 $mg\ ml^{-1}$ bacitracin was used to perfuse the cells at approximately 120 $\mu l\ s^{-1}$. The rate of extracellular acidification was measured during a 30 s interval while perfusion was stopped, followed by a washout period of 60 s. Cells were allowed to equilibrate for 1 h, followed by the addition of 3 μM uridine triphosphate (UTP) for 3 min to confirm cell viability. SRIF was added at 21 min intervals for 10 s, prior to the measurement period. Longer exposure times to SRIF generally produced smaller responses. Concentration-effect (C-E) curves to SRIF were constructed, followed 42 min later by a second C-E curve to SRIF (control) or SRIF analogue. EC_{50} values were calculated for first and second C-E curves, by fitting to a four parameter logistic function, using the curve-fitting programme GraphPad PRISM. In antagonist studies, cells were perfused with media (see above) containing antagonist/inhibitor for 20 min prior to construction of the second C-E curve and remained in the perfusion media throughout this period. Concentration-ratios were calculated by dividing the

SRIF EC_{50} value in the presence of antagonist by the EC_{50} value obtained prior to antagonist administration. The concentration ratio obtained was corrected for spontaneous changes in agonist sensitivity by dividing this ratio by the concentration ratio obtained in the control cup which was always close to unity (see below). For pertussis toxin studies, cells were plated out in media containing 100 ng ml^{-1} pertussis toxin as above. Only one SRIF C-E curve was produced and data were analysed as percentage of the initial UTP response.

Statistical analysis

All IC_{50} and EC_{50} values are geometric means [95% confidence limits] of n observations. All other values are arithmetic means ± s.e.mean. Tests for statistically significant differences were carried out with a Student's unpaired t test, and a probability $P<0.05$ was considered significant.

Materials

Unless otherwise stated, all reagents were purchased from Sigma. Dulbecco's Modified Eagle's Medium, foetal bovine serum and G418 were obtained from Gibco. [^{125}I]-[Tyr^{11}]-SRIF and cyclic AMP [^{125}I] assay system were purchased from Amersham. Bicinchoninic acid (BCA) Protein Assay kit was obtained from Pierce, U.S.A. CGP23996 (cyclo [Asu-Lys-Asn-Phe-Trp-Lys-Thr-Tyr-Thr-Ser]), BIM-23027 (c[N-Me-Ala-Tyr-D-Trp-Lys-Abu-Phe]), BIM-23056 (D-Phe-Phe-Tyr-D-Trp-Lys-Val-Phe-D-Nal-NH2), L-362,855 (c[Aha-Phe-Trp-D-Lys-Thr-Phe]), MK-678 (c[N-Me-Ala-Tyr-D-Trp-Lys-Val-Phe]) and RC-160 (D-Phe-c [Cys-Tyr-D-Trp-Lys-Vat-Cys]-Trp-NH_2) were synthesized by Dr Kitchin's team, Chemistry Division, Glaxo Group Research Ltd. Octreotide, purchased as Sandostatin, was obtained from a pharmaceutical wholesaler.

Results

Ligand affinities for the human sst_1 and sst_2 receptors

The human recombinant sst_1 and sst_2 receptor cDNAs were stably transfected into mouse fibroblast (Ltk$^-$) cells and radiolabelled ligand binding assays were carried out on two clonal cell lines, LSSRI/20 and LSSRII/13, expressing the sst_1 and sst_2 receptor, respectively. Scatchard transformation of competition binding data with SRIF showed that [^{125}I]-[Tyr^{11}]-SRIF binding to both receptors was of high affinity and saturable. Typically, 70% specific binding was observed and no specific binding was detected in non-transfected cells (data not shown). K_d values of 1.52 [0.97–2.4] nM and 0.23 [0.13–0.42] nM (mean values [95% confidence limits]), and B_{max} values of 504 ± 70 fmol mg^{-1} protein and 363 ± 57 fmol mg^{-1} protein (mean values ± s.e.mean) were calculated for [^{125}I]-[Tyr^{11}]-SRIF binding to LSSRI/20 and LSSRII/13 cell membranes, respectively (Figure 1).

Competition studies were carried out with a number of SRIF analogues, including some putatively receptor-selective compounds (Table 1; Figure 2). The sst_2 receptor-selective peptides, MK-678 and BIM-23027, showed no measurable affinity for the sst_1 receptor, but bound with high affinity to the sst_2 receptor. BIM-23056, the putative sst_3 receptor-selective peptide, bound with very low affinity to the sst_1 receptor, but had no measurable affinity for the sst_2 receptor. The sst_5-re-

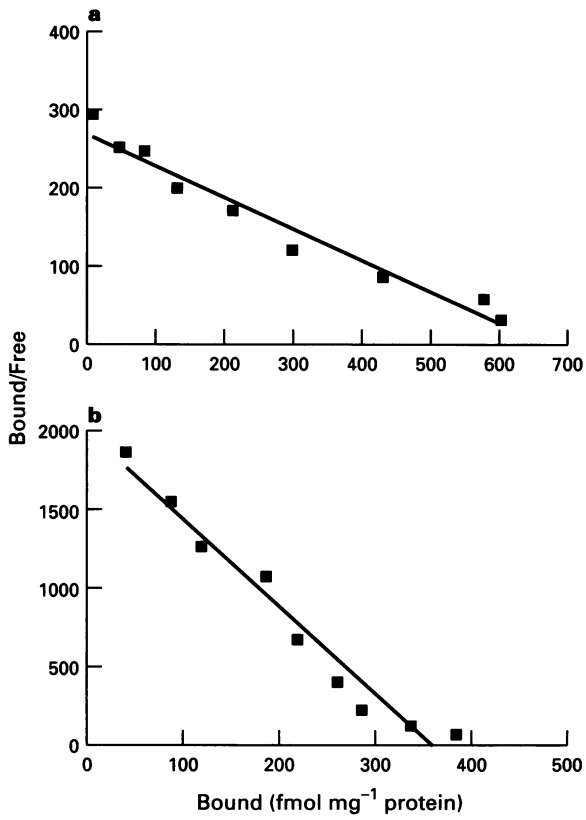

Figure 1 Scatchard plot of [^{125}I]-[Tyr^{11}]-SRIF binding to (a) LSSRI/20 and (b) LSSRII/13 cell membranes. Cell membranes were incubated with 0.03 nM [^{125}I]-[Tyr^{11}]-SRIF and increasing concentrations of SRIF, as described in the text. The ordinate scale represents bound divided by free radioligand expressed as fmol mg^{-1} nM^{-1}. The data are from one representative experiment of five.

Table 1 Competition studies in LSSRI/20 and LSSRII/13 cell membranes with [I^{125}]-[Tyr^{11}]-SRIF

	LSSRI/20		*LSSRII/13*	
	IC_{50} (nM)	*Hill slope*	*IC_{50} (nM)*	*Hill slope*
SRIF	0.68 [0.31–1.47]	0.90 ± 0.05	0.16 [0.11–0.24]	0.98 ± 0.07
SRIF-28	0.64 [0.37–1.13]	0.83 ± 0.07	0.072 [0.012–0.43]	0.85 ± 0.10
BIM-23027	> 1000	–	0.035 [0.006–0.21]	0.74 ± 0.09
MK-678	> 1000	–	0.014 [0.007–0.027]	0.58 ± 0.05
L-362,855	269.1 [191.8–377.5]	0.98 ± 0.19	19.44 [8.0–47.2]	0.73 ± 0.17
[Tyr^{11}]-SRIF	0.43 [0.09–1.99]	0.93 ± 0.08	0.064 [0.024–0.166]	0.79 ± 0.05
[D-Trp^8]-SRIF	0.54 [0.14–2.05]	0.85 ± 0.09	0.04 [0.01–0.13]	0.85 ± 0.06
CGP23996	1.27 [0.94–1.71]	0.61 ± 0.04	0.31 [0.11–0.87]	0.63 ± 0.02
BIM-23056	437.4 [213.6–895.9]	0.88 ± 0.08	> 1000	–

Values shown are mean IC_{50}, nM [95% confidence limits] and mean Hill slopes ± s.e.mean, $n \geq 3$. Note that BIM-23027 and MK-678 displayed no affinity for the sst_1 receptor while BIM-23056 was devoid of quantifiable affinity for the sst_2 receptor.

ceptor selective peptide, L-362,855, also had very low affinity for the sst_1 receptor, but bound with relatively moderate affinity to the sst_2 receptor.

Investigation of the coupling of human sst_1 and sst_2 receptors to changes in cyclic AMP production

The two clonal cell lines, LSSRI/20 and LSSRII/13, were used to investigate the effect of SRIF on basal and forskolin-stimulated increases in cyclic AMP production. The basal levels of cyclic AMP in these cell lines were 13.8 ± 1.0 and 13.6 ± 0.7 pmol cyclic AMP mg^{-1} protein, respectively (values are mean $\pm$ s.e.mean, $n=5$). Incubation with forskolin (10 μM) for 1 min increased cyclic AMP levels by $119 \pm 9\%$ and $106 \pm 12\%$, respectively (Figure 3). SRIF (1 μM) had no effect on basal cyclic AMP production in either cell line and did not affect forskolin-stimulated increases in cyclic AMP (Figure 3).

Extracellular acidfication rate measurements in LSSRI/20 and LSSRII/13 cells

The effects of a number of SRIF analogues on the extracellular acidification rates of the cells expressing sst_1 and sst_2 receptors were investigated. In both cell lines, basal acidification rates for the density of cells used were 100–280 $\mu V\ s^{-1}$ (0.1–0.28 pH units min^{-1}). UTP (3 μM) produced increases in extracellular acidification rates in LSSRI/20 and LSSRII/13 cells (Figure 4) of $43.7 \pm 5.1\%$ ($n=3$) and $59.7 \pm 3.7\%$ ($n=18$) above baseline, respectively. SRIF (0.3–3000 nM) caused concentration-dependent increases in extracellular acidification rates in LSSRII/13 (Figure 4) cells but not LSSRI/20 cells. Maximum increases of $11.3 \pm 0.7\%$ ($n=18$) above baseline were seen for the first SRIF C-E curve using LSSRII/13 cells. Successive C-E curves to SRIF were highly reproducible with EC_{50} values for first and second SRIF C-E curves of 8.1 nM [6.4–10.3] and 6.8 nM [5.6–8.2], respectively ($n=30$).

A series of SRIF analogues were examined for their effects on the rate of extracellular acidification in LSSRII/13 cells expressing the sst_2 receptor (Table 2; Figure 5). The rank order of potencies observed for the peptides used was similar to that seen in the radiolabelled ligand binding assays. The most potent compounds were MK-678 and BIM-23027, while L-362,855 had lower potency than SRIF. Although some of the calculated C-E curve maxima were found to be higher than that of SRIF, none was significantly different. BIM-23056 and the putative somatostatin receptor antagonist, CPP (cyclo(7-aminoheptanoyl-Phe-D-Trp-Lys-Thr[Bzl]), had little or no effect on basal acidification rates. In addition, neither BIM-23056 nor CPP (1 μM) had any significant effect on SRIF-mediated increases in acidification rates (corrected concentration-ratios of 1.8 [0.9–3.5] and 0.3 [0.1–1.4], respectively; Figure 6).

Changes in rates of extracellular acidification of LSSRII/13 cells incubated for at least 18 h with 100 ng ml^{-1} pertussis toxin were also investigated. The responses to UTP were not different either in the absence or presence of pertussis toxin ($67.7 \pm 3.1\%$ and $68.2 \pm 2.0\%$ ($n=4$) above baseline, respectively). In contrast, the maximum response to SRIF was markedly and significantly reduced, from $14.5 \pm 0.8\%$ to $6.4 \pm 1.4\%$ of the UTP response (Figure 7).

Discussion

A number of studies have been undertaken to investigate the operational characteristics of the various recombinant soma-

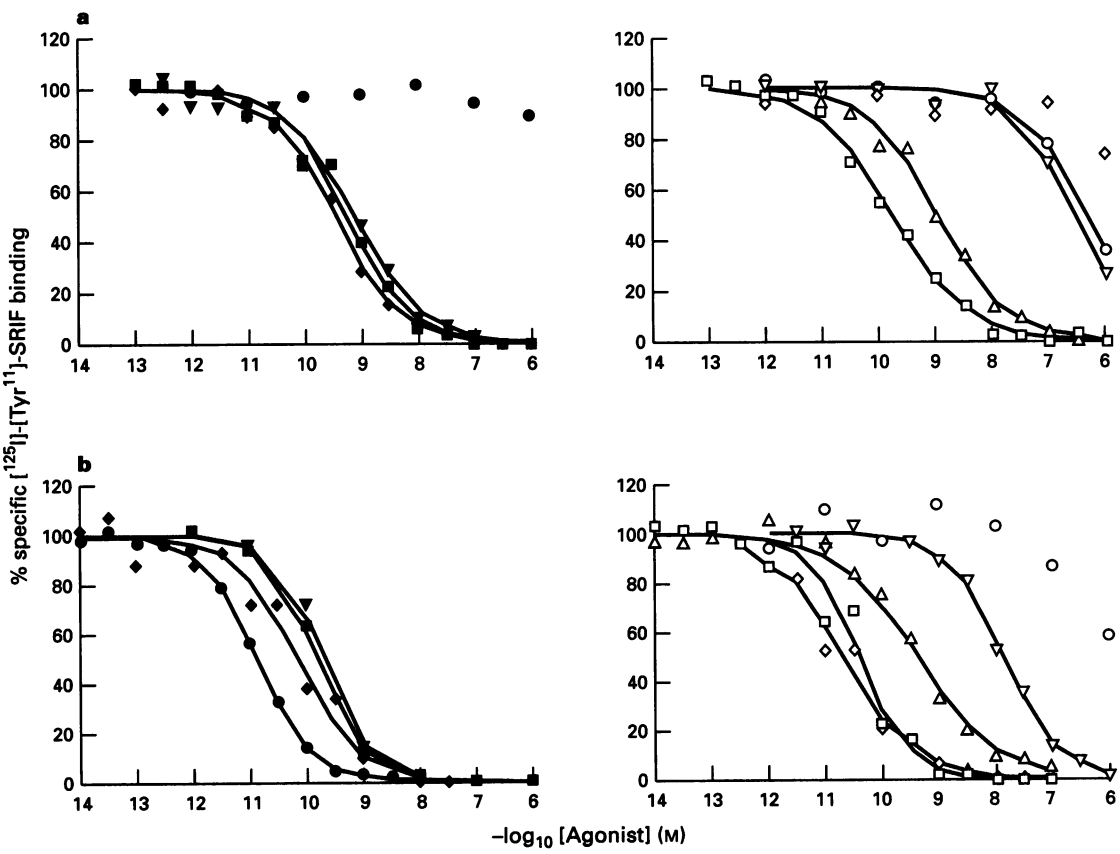

Figure 2 Competition studies of SRIF analogues to (a) LSSRI/20 and (b) LSSRII/13 cell membranes. Cell membranes (20–30 μg protein) were incubated with 0.03 nM [^{125}I]-[Tyr^{11}]-SRIF and increasing concentrations of SRIF (■), SRIF-28 (▼), BIM-23027 (●), [Tyr^{11}]-SRIF (◆), [D-Trp^{8}]-SRIF (□), L-362,855 (▽), BIM-23056 (○), MK-678 (◇) and CGP23996 (△), as described in the text. The data are from one representative experiment of at least three.

tostatin receptor types. These have been carried out in various cell lines using human, rat and mouse receptors. In some studies, receptor types have been compared, which have originated from different species. Even though there is high

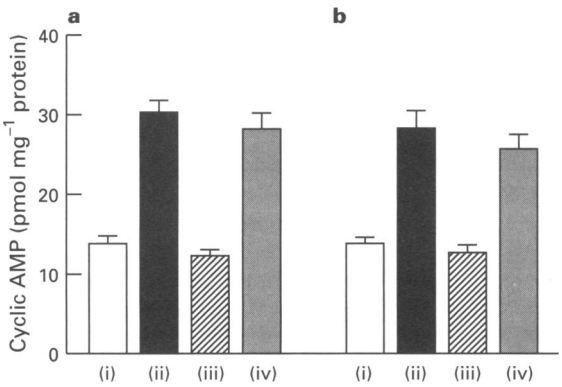

Figure 3 Effect of forskolin in the presence and absence of SRIF on cyclic AMP production in (a) LSSRI/20 and (b) LSSRII/13 cells. Cells were plated out in 24-well cell culture plates and incubated with 10 μM forskolin in the presence or absence of 1 μM SRIF (i) basal cyclic AMP formation; (ii) cyclic AMP formation in the presence of 10 μM forskolin; (iii) basal cyclic AMP formation in the presence of 1 μM SRIF and (iv) cyclic AMP formation in the presence of 10 μM forskolin and 1 μM SRIF. The data shown are the mean ± s.e.mean, $n=5$.

Table 2 Potencies of SRIF analogues at increasing extracellular acidification rates of LSSRII/13 cells in the microphysiometer

	EC_{50} (nM)		*Hill slope*
SRIF [1]	8.1	[6.4–10.3]	1.3 ± 0.1
SRIF [2]	6.8	[5.6–8.2]	1.1 ± 0.1
SRIF-28	25.4	[14.8–43.4]	0.9 ± 0.1
Octreotide	4.9	[2.9–8.4]	1.1 ± 0.1
BIM-23027	0.2	[0.1–0.4]	0.9 ± 0.1
MK-678	0.3	[0.1–0.6]	1.1 ± 0.2
L-362,855	203.6	[65.6–632.4]	1.2 ± 0.1
[D-Trp^8]-SRIF	3.1	[1.8–5.4]	0.9 ± 0.1
Angiopeptin	18.5	[8.9–39.1]	1.3 ± 0.3
CGP23996	17.2	[5.0–58.7]	1.2 ± 0.2
RC-160	9.5	[3.7–24.7]	1.1 ± 0.2
BIM-23056	> 10,000		–
CPP	> 10,000		–

Values shown are mean EC_{50}, nM [95% confidence limits] and mean Hill slopes ± s.e.mean, $n \geq 4$. SRIF [1] and SRIF [2] denote values for the first and second SRIF concentration-effect curves. Note that BIM-23056 and CPP had little activity in concentrations up to 10 μM.

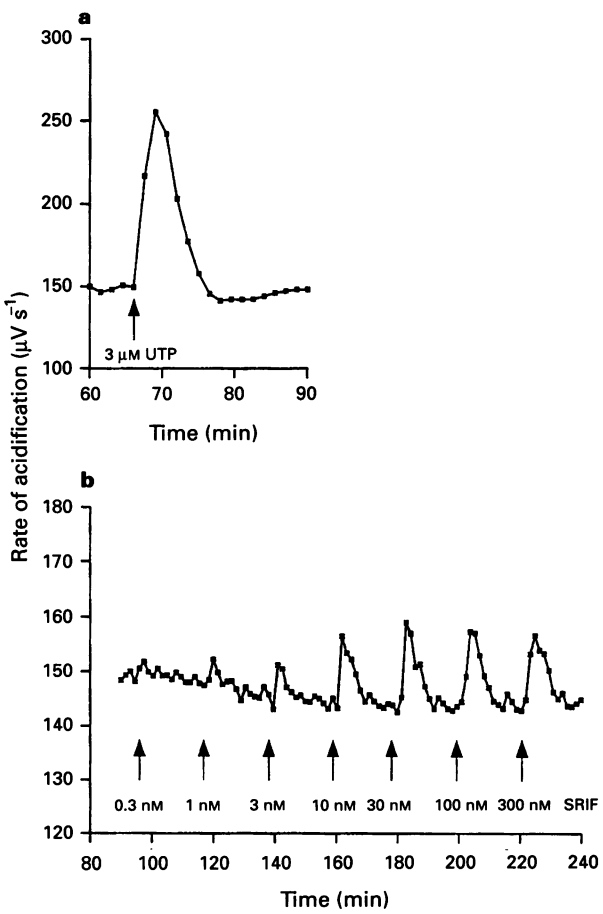

Figure 4 Actual recordings showing the effect of (a) 3 μM UTP and (b) sequential concentrations of SRIF from 0.3–300 nM on the extracellular acidification rates of LSSRII/13 cells measured in the microphysiometer.

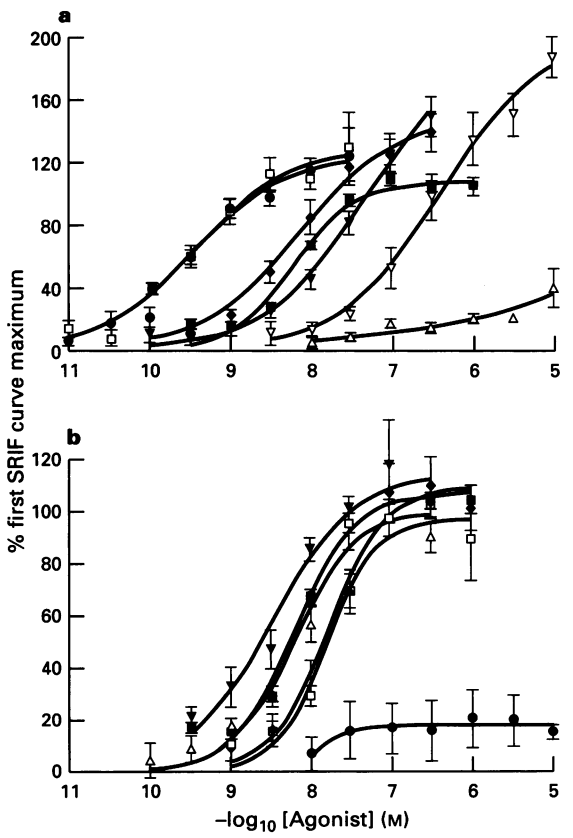

Figure 5 Concentration-effect (C-E) curves to SRIF analogues on LSSRII/13 cells using the microphysiometer to measure extracellular acidification rates. Cells were plated out into microphysiometer cups and assayed as described in the text. Graph (a) shows C-E curves for SRIF (■), SRIF28 (▼), octreotide (◆), BIM-23027 (●), MK-678 (□), BIM-23056 (△) and L-362,855 (▽). Graph (b) shows C-E curves for SRIF (■), [D-Trp^8]-SRIF (▼), angiopeptin (◆), CPP (●), CGP23996 (□) and RC-160 (△). The data shown are the mean ± s.e.mean, $n \geq 4$.

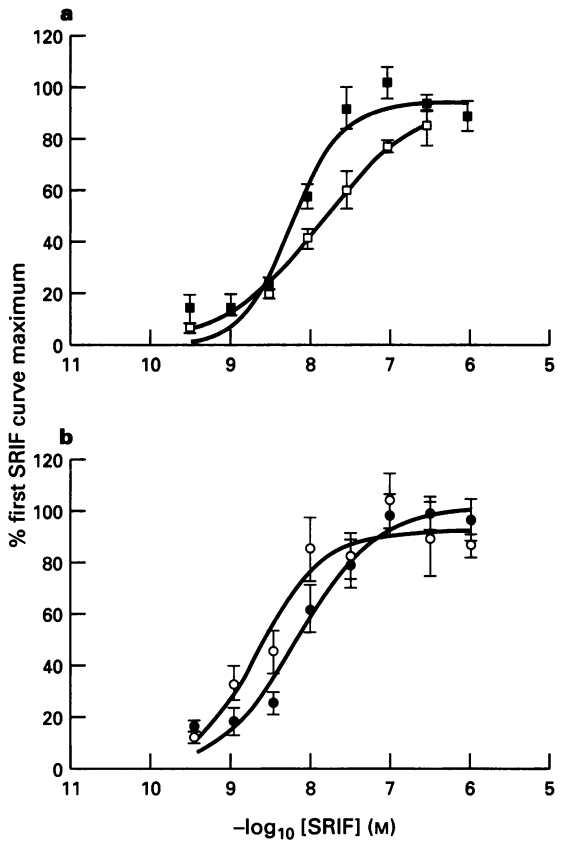

Figure 6 Concentration-effect curves to SRIF on LSSRII/13 cells in the absence (filled symbols) and presence (open symbols) of (a) 1 μM BIM-23056 and (b) 1 μM CPP using the microphysiometer to measure extracellular acidification rates. Cells were plated out into microphysiometer cups and assayed as described in the text. The data shown are the mean ± s.e.mean, $n=5$. Note that neither compound antagonized the effects of SRIF significantly.

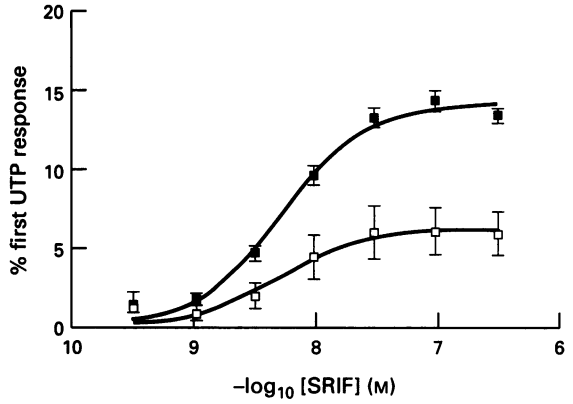

Figure 7 Concentration-effect curves for SRIF on LSSRII/13 cells incubated in the absence (■) and presence (□) of pertussis toxin (100 ng ml^{-1}) using the microphysiometer to measure extracellular acidification rates. Cells were plated out into microphysiometer cups and assayed as described in the text. The data shown are the mean ± s.e.mean, $n=4$.

homology between receptor types from different species, variations in receptor structure could result in differences in ligand binding affinities or G protein coupling. In this study, the human recombinant somatostatin receptors, (sst_1 and sst_2) have been expressed in mouse fibroblast (Ltk$^-$) cells. As well as the quantification of the binding affinities of a number of SRIF analogues, including some compounds which are putatively selective for sst_2, sst_3 or sst_5 receptors (Raynor *et al.*, 1993a,b), we have investigated whether these peptides have functional properties at the human sst_1 and sst_2 receptor.

Two clonal cell lines, LSSRI/20 and LSSRII/13, expressing the human sst_1 and sst_2 receptor, respectively, were used. Scatchard transformation of competition binding data with SRIF suggested that [^{125}I]-[Tyr^{11}]-SRIF binding was saturable and best fitted a one-site model, indicative of an homogeneous population of binding sites in each of these cell lines. SRIF, SRIF28, [Tyr^{11}]-SRIF, [D-Trp^8]-SRIF and CGP23996 all bound with high affinity to both receptor types. However, MK-678, a hexapeptide previously shown to distinguish between $SRIF_1$ and $SRIF_2$ binding sites, had high affinity for the sst_2 receptor in LSSRII/13 cell membranes but not for sst_1 receptors in LSSRI/20 cells. This was also the case for the putative sst_2 receptor-selective hexapeptide, BIM-23027. In this study, MK-678 and BIM-23027 showed approximately the same affinity for the sst_2 receptor expressed in LSSRII/13 cells having a 3–10 fold higher potency than SRIF. However, in a previous study by Raynor and colleagues (Raynor *et al.*, 1993a) BIM-23027 showed a 180 fold higher affinity than MK-678 for the mouse sst_2 receptor expressed in CHO (DG44) cells. It is possible that this difference in the potency of BIM-23027 compared with MK-678 could reflect a species difference. Although the results from our study on the human sst_2 receptor expressed in Ltk$^-$ cells show MK-678 to have a higher affinity than SRIF for the human sst_2 receptor, another study has shown that MK-678 and SRIF have similar potencies on the human sst_2 receptor expressed in CHO-K1 cells (Patel & Srikant, 1994). Whether this difference can be attributed to the different cell line or to the different radioligand used is unknown.

The affinities of the putative sst_3 receptor-selective linear peptide, BIM-23056, and the putative sst_5 receptor selective ligand, L-362,855, for the human sst_1 and sst_2 receptors in LSSRI/20 and LSSRII/13 cells were also measured. Both peptides showed very low affinity for the sst_1 receptor, while L-362,855 showed some affinity for the sst_2 receptor. These findings are also at variance with the first reports on these peptides (Raynor *et al.*, 1993a,b) where BIM-23056 and L-362,855 had no affinity for the sst_1 receptor. The study by Patel & Srikant (1994) also demonstrated low affinity binding of BIM-23056 to the sst_1 receptor. Since there were differences in the cell lines, species, and the radioligand binding protocol used in this study and the others, further investigations would be required to ascertain the reason for the differences reported in the relative affinities of these key peptides. Clearly some circumspection appears necessary in the use of these receptor selective ligands as probes with which to characterize SRIF receptors expressed in native tissue.

Somatostatin receptors have been shown to couple negatively to adenylyl cyclase in a number of different cell types, including CHO, HEK293 and COS cells (Kaupmann *et al.*, 1993; Akbar *et al.*, 1994; Patel *et al.*, 1994) whilst other studies have shown a lack of coupling (Yasuda *et al.*, 1992; Rens-Domiano *et al.*, 1992). In our study, neither sst_1 nor sst_2 receptors expressed in LSSRI/20 and LSSRII/13 cells, respectively, mediated changes in the level of cyclic AMP. A previous study using human sst_1 and mouse sst_2 receptors expressed in mouse fibroblast (Ltk$^-$) cells showed that these receptors coupled negatively to adenylyl cyclase via a pertussis toxin-sensitive mechanism (Hou *et al.*, 1994). There is even conflicting data in the literature from studies where the same receptor type and cell line was used (Rens-Domiano *et al.*, 1992; Kagimoto *et al.*, 1994). The reason for these inconsistencies is unclear. The G protein and adenylyl cyclase complement in the cells used in both sets of studies would be expected to be the same, since the same parental cell line was used. However, it is conceivable that the transfection process itself caused changes to the expression of other proteins necessary for the transduction system in question.

The microphysiometer measures extracellular acidification as a means of monitoring cell metabolism (McConnell *et al.*,

1992). During normal cell metabolism, acidic products are produced and are released into the extracellular environment. Changes in cellular metabolism and/or H^+ exchange due to the binding of hormones or neurotransmitters to cell surface receptors can be monitored by the microphysiometer and this approach was used to investigate the functional characteristics of the human sst_1 and sst_2 receptors in LSSRI/20 and LSSRII/13 cells, respectively.

For both cell lines, UTP produced robust and consistent increases in the rates of extracellular acidification. However, somatostatin caused concentration-dependent increases in acidification rate in LSSRII/13 cells, expressing sst_2 receptors, but not in LSSRI/20 cells, expressing sst_1 receptors. The maximum increases seen with SRIF were approximately 19% of those seen with UTP. Two consecutive C-E curves to SRIF were highly reproducible in a single channel and first curves were also reproducible between channels. A number of SRIF analogues could therefore be compared to SRIF for functional activity at the sst_2 receptor in LSSRII/13 cells using this system. Most of the peptides used displayed agonist actions at this receptor. MK-678 and BIM-23027 were the most potent, having similar EC_{50} values, while L-362,855 had lower potency than SRIF. BIM-23056 and CPP, a putative SRIF receptor antagonist, had little or no effect and neither of these compounds was found to antagonize SRIF-mediated responses.

The relative potencies (EC_{50} values) of the SRIF agonists examined at causing increases in extracellular acidification correlated well with corresponding relative affinity estimates (IC_{50} values) obtained from the ligand binding studies ($r = 0.94$, see Table 2). This suggests that the functional characteristics of the LSSRII/13 cells are due to the transfected sst_2 receptor which effectively couples to a receptor-response system in these cells. To address this further, LSSRII/13 cells were pre-incubated with 100 ng ml^{-1} pertussis toxin prior to analysis in the microphysiometer. The response to UTP was unaffected, but the SRIF-mediated response was reduced by approximately 56%. This indicates that the responses seen with SRIF are, in part at least, mediated by a process involving a pertussis toxin-sensitive G protein. These results also show that the responses seen with UTP and SRIF are likely to be mediated by different transduction systems since the magnitude of the responses and their sensitivities to pertussis toxin were very different. Despite the fact that there was a good correlation between the rank orders of the affinity estimates from the ligand binding studies and the potentices of the agonists in causing increases in extracellular acidification rates, it is noteworthy that in every case the binding estimates (IC_{50} values) were much lower than their equivalent agonist potency estimates (EC_{50} values) assessed by microphysiometry. This implies that the agonists occupied most of the receptor population in order to produce detectable changes in extracellular acidification rates, which in turn suggests that either all the receptors were poorly coupled to the transducer process or that only a proportion was coupled. Alternatively, since agonist binding to the sst_2 receptor is known to be inhibited by GTPγS (Yasuda *et al.*, 1992; Rens-Domiano *et al.*, 1992), it may be that the absence of significant levels of GTP in the binding studies on membranes has converted the transfected sst_2 receptors to a high affinity state.

The studies with pertussis toxin are also interesting in the light of another study using human sst_1 and mouse sst_2 receptors expressed in mouse fibroblast (Ltk^-) cells (Hou *et al.*, 1994) where the recovery of intracellular pH in acid-loaded cells was monitored with the fluorescent pH-sensitive dye, BCECF. The rate of recovery was slowed by SRIF in cells expressing the sst_1 receptor but not sst_2 receptors, which is very different from the finding in this study, where increases in acidification were observed in cells expressing the sst_2 receptor but not the sst_1 receptor. It is unlikely that these differences were due to marked differences in Na^+/H^+ exchange activity since the basal extracellular acidification rates observed in our study (0.1–0.28 pH units min^{-1}) were similar to basal Na^+/H^+ exchange activity seen by Hou and colleagues (1994). The response that they observed was attributed to the inhibition of the Na^+/H^+ exchanger by SRIF since the effect of SRIF was inhibited in the absence of extracellular Na^+ and in the presence of ethylisopropylamiloride, and was pertussis toxin-insensitive (Hou *et al.*, 1994). In our study the continuous application of 1 mM amiloride to LSSRII/13 cells resulted in an initial decrease, but not an abolition, in the rate of extracellular acidification, followed by a gradual recovery in rate (unpublished observation). The SRIF-mediated increases in acidification rates were reduced in the presence of amiloride as well as the absence of extracellular Na^+ (unpublished observations). Further studies are required to determine the precise mechanism by which SRIF caused an increase in extracellular acidification in LSSRII/13 cells following activation of sst_2 receptors, but one possible interpretation of our findings is that SRIF stimulates rather than inhibits Na^+/H^+ exchange. Alterntively sst_2 receptor activation may have simply increased the metabolic rate of the cells.

It is interesting to note that the sst_1 receptors expressed in LSSRI/20 cells do not appear to be coupled to either of the two transduction systems investigated in this study, i.e. the inhibition of adenylyl cyclase or the modification of extracellular acidification rates. In a number of other studies, sst_1 receptor has been found to negatively couple to adenylyl cyclase in various cell types, including mouse fibroblast (Ltk^-) cells (Kaupmann *et al.*, 1993; Patel *et al.*, 1994; Hou *et al.*, 1994) and to positively couple to phospholipase C, leading to Ca^{2+} mobilization, though the magnitude of this response was small (Akbar *et al.*, 1994). Nevertheless we have shown that there is a pertussis toxin-sensitive G protein in LSSRII/13 cells which the sst_2 receptor is able to activate, leading to the SRIF-mediated increases in extracellular acidification. The present study does not allow one to determine whether the residual acidification response in the presence of pertussis toxin is mediated via a pertussis toxin-insensitive G protein since inactivation of G_i and G_O may have been incomplete. However, it appears that the sst_1 receptor in LSSRI/20 cells is either unable to interact with these G proteins, or that the G protein expression is suppressed.

In summary, the two clonal cell lines LSSRI/20 and LSSRII/13, expressing the human sst_1 and sst_2 receptors, respectively, have been used to study the operational selectivity of a number of SRIF analogues for these two receptor types. Although the absolute affinities of some of these peptides has been brought into question by this study, MK-678, BIM-23027 and L-362,855 were shown to bind selectively to the sst_2 receptor rather than the sst_1 receptor. The lack of high affinity binding at either receptor by BIM-23056 has also been confirmed. Importantly, by measuring extracellular acidification rates, the agonist characteristics of these peptides has been demonstrated on the recombinant human sst_2 receptor. However, the precise transduction events involved remain to be determined.

References

AKBAR, M., OKAJIMA, F., TOMURA, H., MAJID, M.S., YAMADA, Y., SEINO, S. & KONDO, Y. (1994). Phospholipase C activation and Ca^{2+} mobilization by cloned human somatostatin subtypes 1-5 in transfected COS-7 cells. *FEBS Lett.*, **348**, 192–196.

BARBER, D.L., MCGUIRE, M.E. & GANZ, M.B. (1989). β-adrenergic and somatostatin receptors regulate Na-H exchange independent of cAMP. *J. Biol. Chem.*, **264**, 21038–21042.

BUELL, G., SCHULZ, M.F., ARKINSTALL, S.J., MAURY, K., MISSOTTEN, M., ADAMI, N., TALABOT, F. & KAWASHIMA, E. (1992). Molecular characterization, expression and localization of human neurokinin-3 receptor. *FEBS Lett.*, **299**, 90–95.

CASTRO, S.W., BUELL, G., FENIUK, W. & HUMPHREY, P.P.A. (1994). The expression and characterization of the human SSTR1 and SSTR2 receptors in mouse fibroblast cell lines. *Br. J. Pharmacol.*, **113,** 133P.

CASTRO, S.W., FENIUK, W. & HUMPHREY, P.P.A. (1995). The human somatostatin sst_2 receptor mediates increases in the rate of intracellular acidification in a mouse fibroblast (Ltk^-) cell line. *Br. J. Pharmacol.*, **116,** 20P.

EPELBAUM, J. (1986). Somatostatin in the nervous system: physiology and pathological modifications. *Prog. Neurobiol.*, **27,** 63–100.

FENIUK, W., DIMECH, J., JARVIE, E.M. & HUMPHREY, P.P.A. (1995). Further evidence from functional studies for somatostatin receptor heterogeneity in guinea-pig isolated ileum, vas deferens and right atrium. *Br. J. Pharmacol.*, **115,** 975–980.

HENIKOFF, S. (1984). Unidirectional digestion with exonuclease III creates targeted breakpoints for DNA sequencing. *Gene*, **28,** 351–359.

HOU, C., GILBERT, R.L. & BARBER, D.L. (1994). Subtype-specific signalling mechanisms of somatostatin receptors SSTR1 and SSTR2. *J. Biol. Chem.*, **269,** 10357–10362.

HOYER, D., BELL, G.I., BERELOWITZ, M., EPELBAUM, J., FENIUK, W., HUMPHREY, P.P.A., O'CARROLL, A.M., PATEL, Y.C., SCHONBRUNN, A., TAYLOR, J.E. & REISINE, T. (1995). Classification and nomenclature of somatostatin receptors. *Trends Pharmacol. Sci.*, **16,** 86–88.

JAKOBS, K.H., AKTORIES, K. & SCHULTZ, G. (1983). A nucleotide regulatory site for somatostatin inhibition of adenylate cyclase in S49 lymphoma cells. *Nature*, **303,** 177–178.

KAGIMOTO, S., YAMADA, Y., IHARA, Y., YASUDA, K., KOZASA, T., IMURA, H., SEINO, S. & SEINO, Y. (1994). Human somatostatin receptor, SSTR2, is coupled to adenylyl cyclase in the presence of Giα1 protein. *Biochem. Biophys. Res. Commun.*, **202,** 1188–1195.

KAUPMANN, K., BRUNS, C., HOYER, D., SEUWEN, K. & LÜBBERT, H. (1993). Distribution and second messenger coupling of four somatostatin receptor subtypes expressed in brain. *FEBS Lett.*, **331,** 53–59.

KOCH, B.D., DORFLINGER, L.J. & SCHONNBRUNN, A. (1985). Pertussis toxin blocks both cAMP-mediated and cAMP-independent actions of somatostatin. *J. Biol. Chem.*, **260,** 13138–13145.

LEWIS, D., WEIGHT, F. & LUINI, A. (1986). A guanine nucleotide-binding protein mediating the inhibition of voltage-dependent calcium current by somatostatin in a pituitary cell line. *Proc. Natl. Acad. Sci. U.S.A.*, **83,** 9035–9039.

LIEBOW, C., REILLY, C., SERRANO, M. & SCHALLY, A. (1989). Somatostatin analogues inhibit growth of pancreatic cancer by stimulating tyrosine phosphatase. *Proc. Natl. Acad. Sci. U.S.A.*, **86,** 2003–2008.

MCCONNELL, H.M., OWICKI, J.C., PARCE, J.W., MILLER, D.L., BAXTER, G.T., WADA, H.G. & PITCHFORD, S. (1992). The Cytosensor Microphysiometer: Biological applications of silicon technology. *Science*, **257,** 1906–1912.

MCKEEN, E.S., FENIUK, W. & HUMPHREY, P.P.A. (1994). Mediation by $SRIF_1$ receptors of the contractile action of somatostatin in rat isolated distal colon: studies using some novel SRIF analogues. *Br. J. Pharmacol.*, **113,** 628–634.

MCPHERSON, G.A. (1985). Analysis of radioligand binding experiments: a collection of computer programmes for the IBM PC. *J. Pharmacol. Methods*, **14,** 213–228.

MUNSON, P.J. & RODBARD, D. (1980). LIGAND: a versitile, computerized approach for the characterization of ligand binding systems. *Anal. Biochem.*, **107,** 220–239.

PAGE, M.J. (1988). Expression of foreign genes in mammalian cells. In *Methods in Molecular Biology*, Vol. 4: New Nucleic Acid Techniques. ed. Walker, J.M. pp. 380–382. Clifton, New Jersey: Humana Press.

PATEL, Y.C., GREENWOOD, M.T., WARSZYNSKA, A., PANETTA, R. & SRIKANT, C.B. (1994). All five cloned human somatostatin receptors (hSSTR1-5) are functionally coupled to adenylyl cyclase. *Biochem. Biophys. Res. Commun.*, **198,** 605–612.

PATEL, Y.C. & SRIKANT, C.B. (1994). Subtype selectivity of peptide analogues for all five cloned human receptors (hsstr1-5). *Endocrinology*, **135,** 2814–2817.

RAYNOR, K., MURPHY, W.A., COY, D.H., TAYLOR, J.E., MOREAU, J.-P., YASUDA, K., BELL, G.I. & REISINE, T. (1993a). Cloned somatostatin receptors: identification of subtype-selective peptides and demonstration of high affinity binding of linear peptides. *Mol. Pharmacol.*, **43,** 838–844.

RAYNOR, K., O'CARROLL, A.M., KONG, H., YASUDA, K., MAHAN, L.C., BELL, G.I. & REISINE, T. (1993b). Characterization of cloned somatostatin receptors SSTR4 and SSTR5. *Mol. Pharmacol.*, **44,** 385–392.

RAYNOR, K. & REISINE, T. (1989). Analogues of somatostatin selectively label distinct subtypes of somatostatin receptors in rat brain. *J. Pharmacol. Exp. Ther.*, **251,** 510–517.

RAYNOR, K., WANG, H.L., DICHTER, M. & REISINE, T. (1991). Subtypes of somatostatin receptors couple to multiple cellular effector systems. *Mol. Pharmacol.*, **40,** 248–253.

REICHLIN, S. (1983). Somatostatin. *New Engl. J. Med.*, **309,** 1495–1501, 1556–1563.

RENS-DOMIANO, S., LAW, S.F., YAMADA, Y., SEINO, S., BELL, G.I. & REISINE, T. (1992). Pharmacological properties of two cloned somatostatin receptors. *Mol. Pharmacol.*, **42,** 28–34.

REUBI, J.C. (1984). Evidence for two somatostatin-14 receptor types in rat brain cortex. *Neurosci. Lett.*, **49,** 259–263.

VIGUERIER, N., TAHIN-JOUTI, N., AYRAL, A.M., CAMBILLAM, C., SCEMAMA, J.L., BASTIÉ, M.J., KRUHTESEN, S., ESTÈIRE, J.P., PRADAYROL, L., SUSINI, C. & VAYSSE, N. (1989). Direct inhibitory effects of a somatostatin analogue, SMS 201–995, on AR4-2J cell proliferation via pertussis toxin-sensitive guanosine triphosphate-binding protein-independent mechanism. *Endocrinology*, **124,** 1017–1025.

YAMADA, Y., POST, S.R., WANG, K., TAGER, H.S., BELL, G.I. & SEINO, S. (1992). Cloning and functional characterization of a family of human and mouse somatostatin receptors expressed in brain, gastrointestinal tract and kidney. *Proc. Natl. Acad. Sci. U.S.A.*, **89,** 251–255.

YAMASHITA, N., SHIBUYA, N. & OGATA, E. (1987). Hyperpolarization of the membrane potential caused by somatostatin in dissociated human putuitary adenoma cells that secrete growth hormone. *Proc. Natl. Acad. Sci. U.S.A.*, **83,** 6198–6202.

YASUDA, K., RENS-DOMIANO, S., BREDER, C.D., LAW, S.F., SAPER, C.B., REISINE, T. & BELL, G.I. (1992). Cloning of a new somatostatin receptor, SSTR3, coupled to adenylyl cyclase. *J. Biol. Chem.*, **267,** 20422–20428.

(Received August 17, 1995
Revised October 5, 1995
Accepted October 20, 1995)